LBL-27774

Center for Advanced Materials

CAM

To be presented at the ASME Winter Annual Conference,
San Francisco, CA, December 10–14, 1989, and
to be published in *Journal of Electronic Packaging*

Isothermal Fatigue Behavior of Sn-Pb Solder Joints

T.S.E. Summers and J.W. Morris, Jr.

September 1989

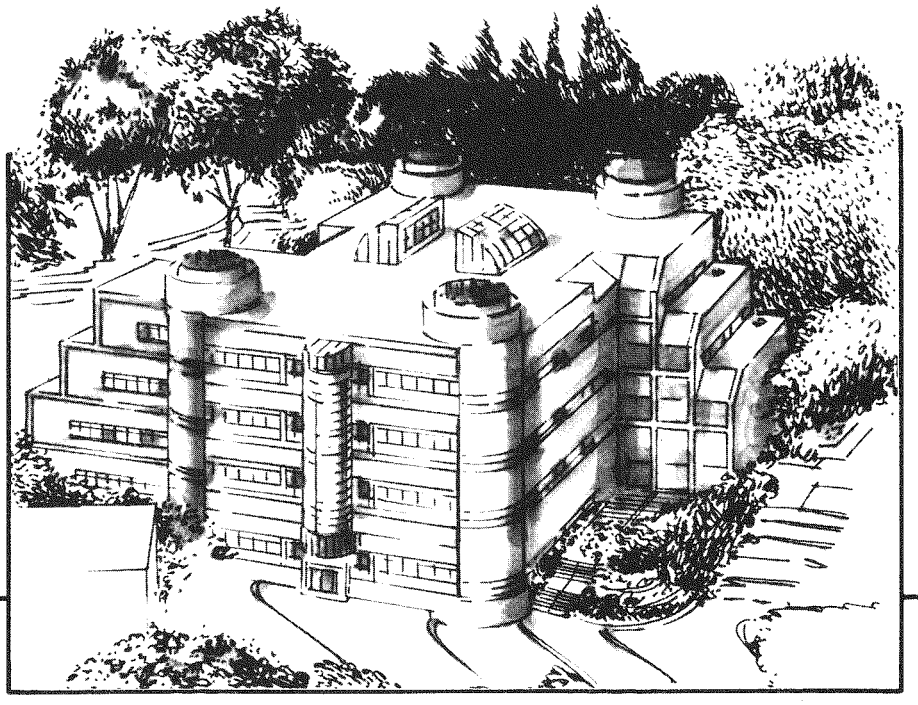

Materials and Chemical Sciences Division

Lawrence Berkeley Laboratory • University of California

ONE CYCLOTRON ROAD, BERKELEY, CA 94720 • (415) 486-4755

Prepared for the U.S. Department of Energy under Contract DE-AC03-76SF00098

LBL--27774

DE90 003280

Isothermal Fatigue Behavior of Sn-Pb Solder Joints

T. S. E. Summers and J. W. Morris, Jr.

Center for Advanced Materials
Materials and Chemical Sciences Division
Lawrence Berkeley Laboratory
1 Cyclotron Road
Berkeley, CA 94720
and
Department of Materials Science and Mineral Engineering
University of California

September 1989

This work is supported by the Director, Office of Energy Research, Office of Basic Energy Science, Material Sciences Division of the U. S. Department of Energy under Contract No. *DE-AC03-76SF00098*

Isothermal Fatigue Behavior of Sn-Pb Solder Joints

T.S.E. Summers and J.W. Morris, Jr.

Center for Advanced Materials, Lawrence Berkeley Laboratory and
Department of Materials Science and Mineral Engineering,
University of California at Berkeley

Isothermal fatigue data were collected for the compositions 5Sn-95Pb, 20Sn-80Pb, 40Sn-60Pb, 50Sn-50Pb and 63Sn-37Pb within the binary Sn-Pb system. All of these compositions are commercially available and include those most commonly used. Because Sn-rich solders are rarely used, they were not investigated here. The fatigue life was defined by a 30% load drop. The solders were tested in a double shear configuration joined to copper at 75°C. The displacement rate chosen was 0.01mm/min, which corresponds to a strain rate of 1.5×10^{-4} s^{-1} for our specimen configuration, over a 10% plastic strain range. Additionally, the microstructural changes during fatigue are presented. The various solder compositions studied exhibit strikingly different as-solidified microstructures. These differences are discussed in terms of their effect on the isothermal joint failure mechanism and joint isothermal fatigue life.

INTRODUCTION

Considerable interest in tin (Sn)-lead (Pb) solders has arisen in the electronics industry where new technologies are requiring leadless solder joints to provide mechanical support as well as electrical contact. Due to the differences in the thermal expansion coefficients of materials joined on either side of a solder joint, these leadless joints must resist shear straining upon thermal cycling. The solder property of interest, then, is thermal fatigue resistance in shear.

Often solder applications require solders of different melting points. Tin-lead solders containing about 5% Sn with a melting point of about 300°C and near-eutectic solders with a 183°C melting point are often chosen in these instances. Published solder properties [1-4], however, suggest that other Sn-Pb solders may offer better fatigue resistance.

A lot of fatigue data exists for the near-eutectic Sn-Pb alloys. In addition to contributing to this database, Solomon [5-8] gives a good review of it. The use of this data in predicting the fatigue lives of actual joints operating under typical service conditions, however, is still unreliable. Because an accelerated fatigue test will only be valid if it reproduces the fatigue mechanisms seen in service, an understanding of the mechanisms and microstructural changes associated with fatigue must be well understood. In addition to aiding the design and evaluation of accelerated tests, an understanding of fatigue mechanisms can suggest more systematic approaches to improving the fatigue resistance of these alloys. For these reasons, understanding the mechanisms of and microstructural evolution during fatigue is at least as important as actual fatigue data. Most of the

microstructural studies that have been done have involved near-eutectic Sn-Pb alloys[1,2,12-17], but some work has been done on 5Sn-95Pb[9-11,17]. Very few microstructural observations exist for other Sn-Pb compositions.

Previous work in this laboratory [17] and elsewhere [1,2,13,18] has shown that the mechanism of thermal shear fatigue failure in near-eutectic Sn-Pb solders involves the development of a coarsened band. Further studies have shown that the same general mechanism is involved in isothermal fatigue and in creep of these alloys [15]. Based on observations made recently in this laboratory of microstructural changes occurring during creep of eutectic (63Sn-37Pb) solder, a mechanism was proposed for growth of this coarsened band [16]. This mechanism involves the nonuniform deformation seen to occur in as-cast eutectic Sn-Pb solder and stress concentrations in the joint. Specifically, the solder will recrystallize locally in a region where it is deforming near one of the stress concentrations in the joint. This locally-recrystallized region is softer than the surrounding as-cast material and hence acts as a mode II crack concentrating the deformation ahead of it. The region ahead of the "crack tip" will then recrystallize thus propagating the coarsened band until it has traversed the joint. At that point, deformation will concentrate within this narrow coarsened region with subsequent failure occurring there. Subtle differences in the failure mechanism occurring in fatigue may exist and should be investigated.

Thermal fatigue is a complicated test to perform as well as analyze. The testing parameters are not easily controlled independently. For example, the strain depends on the temperature cycle, and the strain rate depends on the heating and cooling rates which often are not the same. As stated above, previous work has shown that the same failure mechanism is involved in isothermal fatigue as in thermal fatigue. Isothermal fatigue, however, is much better than thermal fatigue for studying failure mechanisms and microstructural changes because the strain, temperature and strain rate are independently variable. In addition, an objective lifetime may be obtained by looking at the drop in load with cycling. Isothermal fatigue is often proposed for accelerated fatigue testing. Hence, the mechanisms involved in isothermal fatigue are themselves of interest. For these reasons, isothermal fatigue was chosen for studying the fatigue mechanisms of Sn-Pb solders. The subtle details of any conclusions made will eventually have to be verified by thermal fatigue.

For these preliminary studies, a relatively large strain (10%) and high temperature (75°C) were chosen. This choice of strain amplitude and temperature allows an overview of the failure mechanisms to be investigated in a relatively short time. Previous work at high strains has shown that the failure mechanisms are the same as those seen in real joints at much lower strains [14,15,17]. Of course, this initial study will be followed by an investigation of fatigue failures at smaller strain amplitudes.

EXPERIMENTAL

Five Sn-Pb compositions were made by combining 99.9% pure Pb with commercial bar 63Sn-37Pb solder. Ingots of all but the eutectic alloy were made by combining the

appropriate amounts of each material and heating them to 50°C above the melting point of Pb (i.e. to 375°C).

The specimen used is shown in Figure 1. It was designed at this laboratory [19] to shear the two central solder joints when the specimen is placed in uniaxial tension/compression as shown. It is made by bolting together polished Cu plates of the specified thicknesses separated by 0.5-mm (20-mil) wire. This Cu block is then coated with flux and dunked in solder of the desired composition at 100°C above its melting point. The Cu block/solder/crucible assembly is quenched in ice water. Machining and slicing of the block results in about ten specimens. The joint thicknesses and lengths are measured with a travelling microscope to an accuracy of at least ±0.01mm.

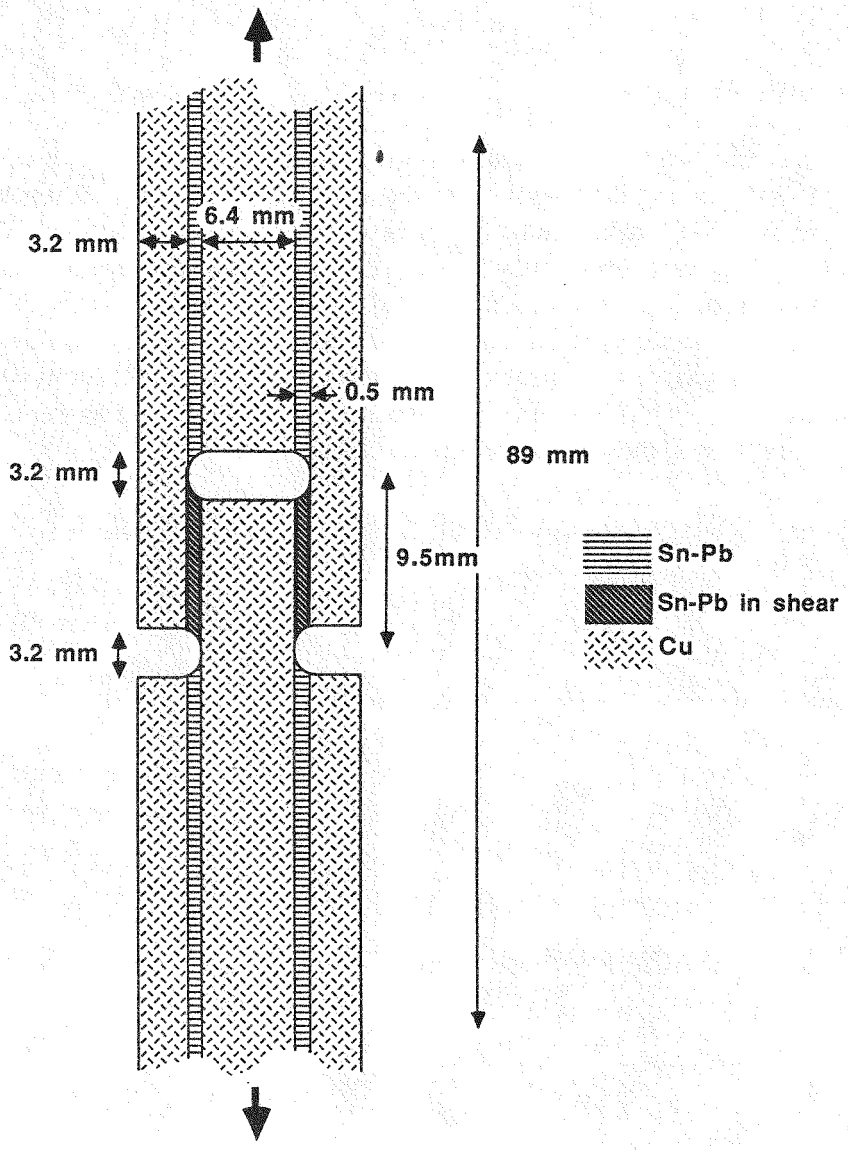

Figure 1. Schematic Illustration of the double shear specimen used for testing solder joints in fatigue. The surrounding material is copper..

Fatigue testing was done by stroke control using a custom-built load frame described previously [10,19]. The quarter-cycle displacement was 0.05mm (2 mil) which after subtraction of the measured machine compliance resulted in a 10% strain amplitude. The displacement rate was 0.01mm/min (about $1.5 \times 10^{-4} s^{-1}$ strain rate), and the temperature was maintained at 75 ± 2°C in oil during testing.

Preparation of the specimens for metallographic examination involved polishing to 0.05μm Al_2O_3 powder using standard metallographic techniques. A final polish was done using a slightly alkaline silica colloidal suspension. The 5Sn-95Pb samples were also chemically polished and etched using a technique described elsewhere [20,21]. Specimen microstructures were examined optically.

RESULTS

Initial Microstructures

Typical initial microstructures are shown in Figures 2 and 3. The eutectic-rich alloys: 63Sn-37Pb, 50Sn-50Pb and 40Sn-60Pb are shown together in Figure 2 while the Pb-rich 20Sn-80Pb and 5Sn-95Pb alloys are shown in Figure 3. In the eutectic solder joints, a colony structure described previously [14,16] for as-cast near-eutectic Sn-Pb alloys is observed as can be seen in Figure 2(a) and (b). The eutectic regions of the 50Sn-50Pb and the 40Sn-60Pb microstructures shown in Figure 2(c)-(f) is somewhat similar to the as-cast eutectic alloy except that it is coarser and has a less well-defined colony structure with smaller over-all colony size. The Pb-rich proeutectic phase forms as dendrites in these alloys and appears to be somewhat heavily precipitated with Sn.

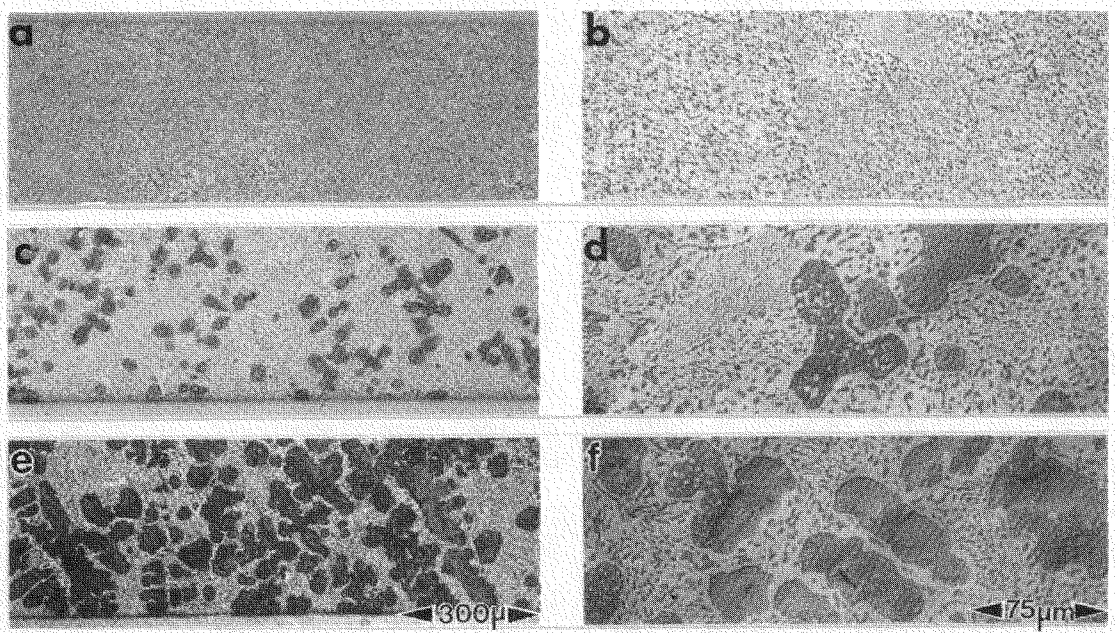

Figure 2. Micrographs showing typical as-cast microstructures of the eutectic-rich alloys: a) and b)63Sn-37Pb, c) and d)50Sn-50Pb and e) and f)40Sn-60Pb. (Top six figures of **XBB 898-6546**)

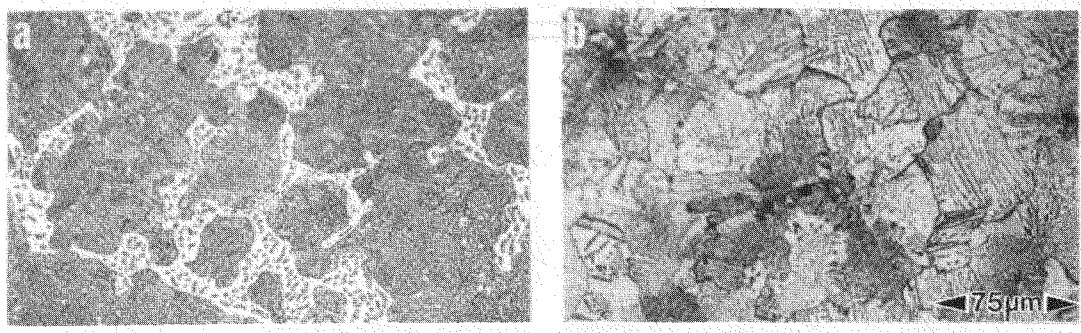

Figure 3. Typical Pb-rich a)20Sn-80Pb and b)5Sn-95Pb as-cast microstructures. (Bottom two figures of **XBB 898-6546**)

The 20Sn-80Pb microstructure shown in Figure 3(a) is almost completely made up of the Pb proeutectic phase. Along the Pb phase boundaries is a relatively thin film of eutectic material which formed during the final stages of solidification.

Lead containing 5%Sn is a single-phase solid solution above about 75°C [22], but at room temperature, 5Sn-95Pb is supersaturated with Sn. Most as-cast 5Sn-95Pb solder joint microstructures show Sn precipitates with the cellular structure seen in Figure 3(b) [22].

Fatigue Data

The fatigue test results are shown in Figures 4 and 5. In all the fatigue tests performed for this study, the stress amplitudes never stabilized during fatigue cycling; they dropped for the most part linearly with the number of cycles. Typical plots of the stress amplitude vs. the number of cycles for each composition are shown in Figure 4. The fatigue life as a

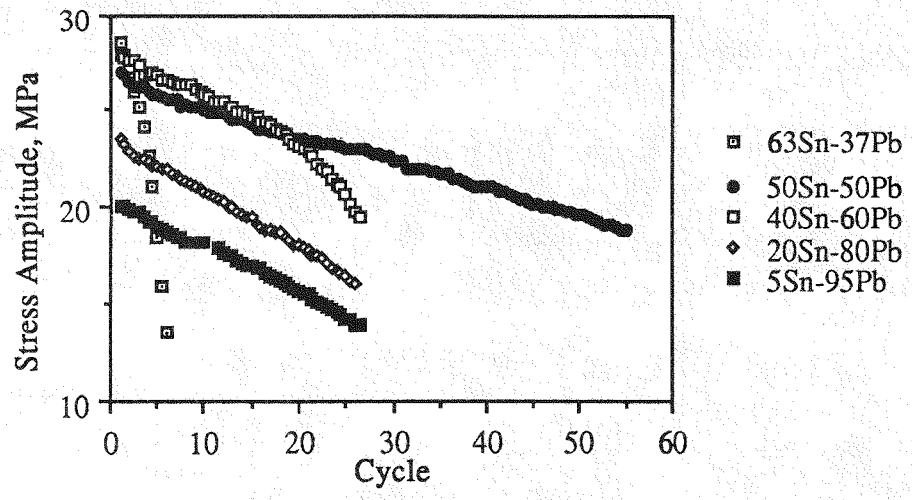

Figure 4. Graph of the cyclic stress amplitude vs. the number of fatigue cycles for the five solder compositions tested.

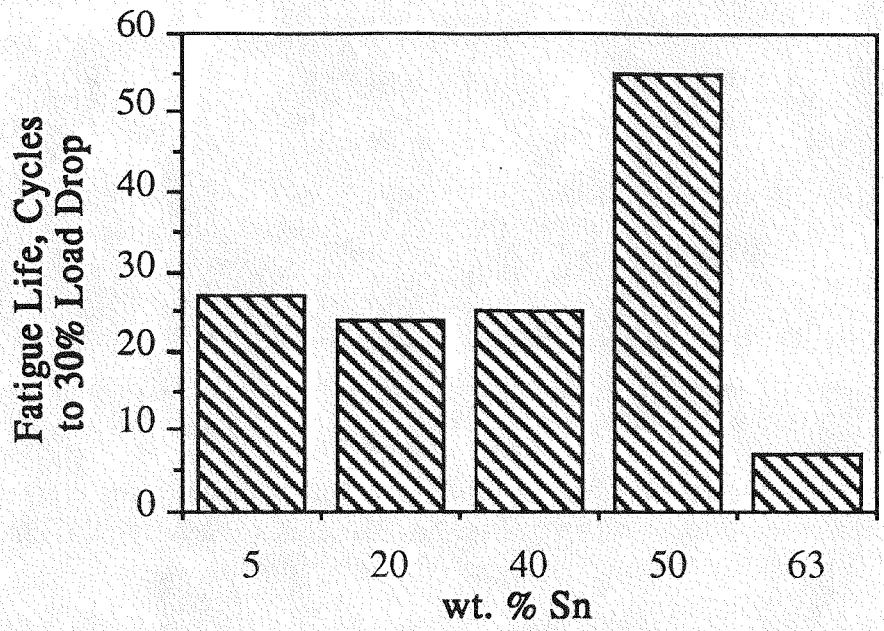

Figure 5. Graph showing the relative fatigue lives of the five solder compositions tested.

function of composition is shown in Figure 5. The 50Sn-50Pb solder showed the best fatigue resistance followed by 40Sn-60Pb, 20Sn-80Pb and 5Sn-95Pb which were about the same. The eutectic 63Sn-37Pb solder showed the least resistance to fatigue failure under the testing conditions used.

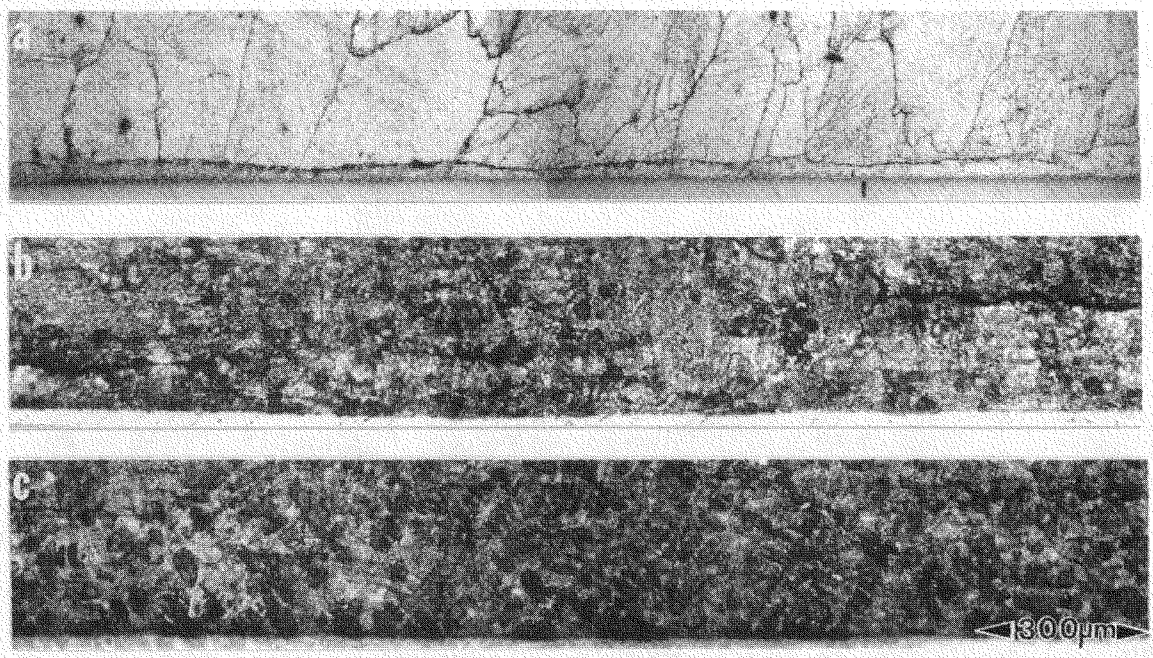

Figure 6. Micrograph showing the surface relief following fatigue of a)63Sn-37Pb,b)50Sn-50Pb and c)40Sn-60Pb joints. (Top three figures of **XBB 898-6766**)

As-Deformed Microstructures

Micrographs of as-deformed polished samples for the three eutectic-rich compositions tested are shown in Figure 6. Figure 6(a) shows deformation in a eutectic sample. As has been shown to be the case for creep of eutectic solder joints [16], eutectic solders deform primarily in the colony boundaries under these loading conditions. The "failed" specimen of Figure 6(a) shows a band of concentrated deformation along the bottom of the joint. The deformation apparent along colony boundaries in the rest of the joint presumably occurred primarily before formation of the band running through the joint. Specimens made of the other two eutectic-rich compositions deformed much more uniformly as shown in Figures 6(b) and (c). Deformation in the 40Sn-60Pb and 50Sn-50Pb alloys, however, is still nonuniform to some extent. The overall deformation looks more uniform largely because the colony size is smaller.

Micrographs of the repolished eutectic-rich specimens are shown in Figure 7. As shown in Figure 7(a), a distinct coarsened band is evident in the fatigued eutectic alloy. The 50Sn-50Pb sample shown in Figure 7(b) and the 40Sn-60Pb sample of Figure 7(c) also have coarsened regions, but they are much less distinct and had not propagated in as far as those seen in the eutectic samples. In none of the joints tested had this coarsened band propagated completely through. Cracking, however, had already begun in most of the coarsened bands. Typical fine cracks are shown in Figure 8.

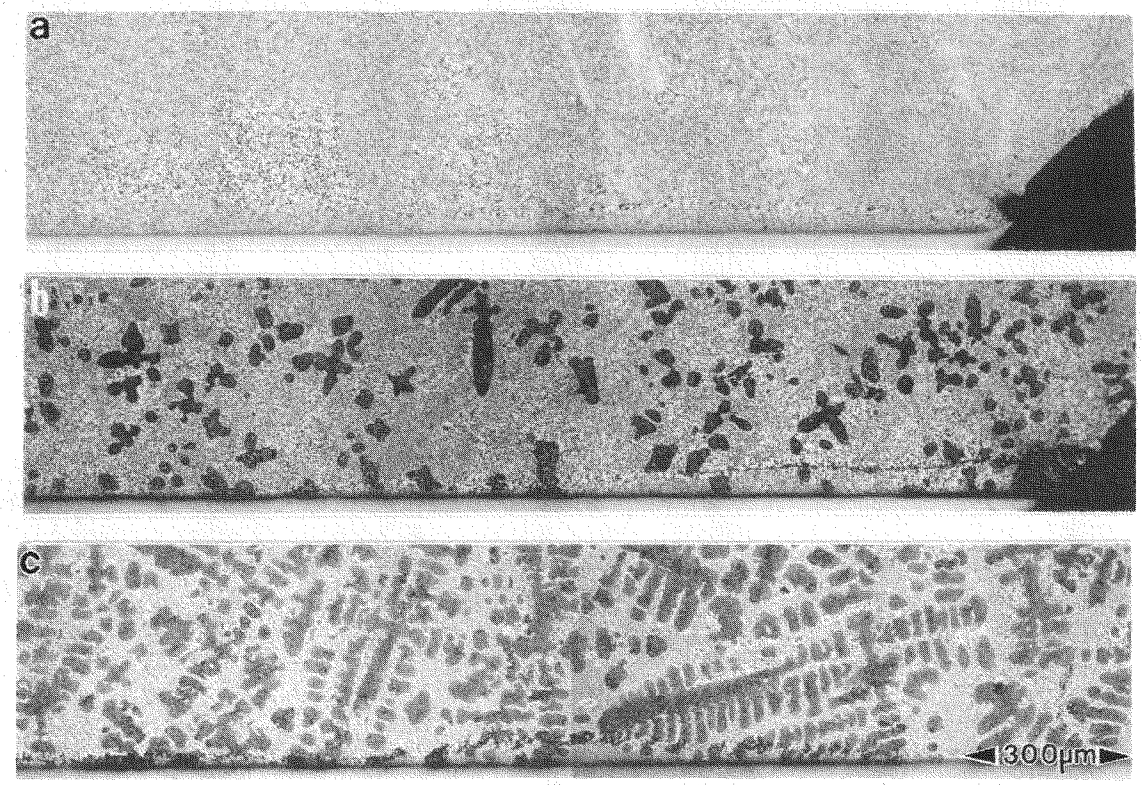

Figure 7. Micrograph of polished a)63Sn-37Pb, b)50Sn-50Pb and c)40Sn-60Pb joints that have been fatigued. (Left three figures of **XBB 898-6545**)

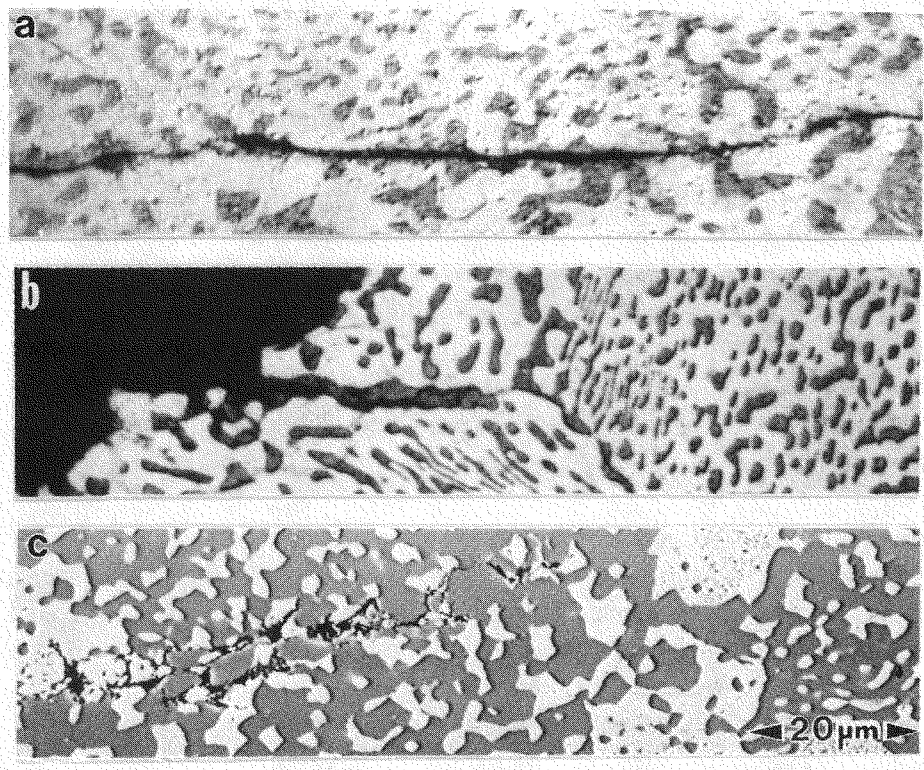

Figure 8. a)Optical micrograph of a crack in the coarsened band of a fatigued 50Sn-50Pb joint, b)Optical micrograph of a crack in the coarsened band of a fatigued 63Sn-37Pb joint, c)SEM micrograph of the end of a crack within the coarsened band of a fatigued 50Sn-50Pb solder joint. Note that while Pb appears dark in optical micrographs, it appears light in an SEM micrograph. **(XBB 899-7331)**

Micrographs of the Pb-rich alloys repolished after fatigue are shown in Figure 9. These specimens did not fail by the formation of a coarsened region. Instead, they failed by cracking in the Pb phase. Failure in the 20Sn-80Pb alloy appears to be accompanied by a break up of the eutectic microstructure initially present at Pb phase boundaries as shown in Figure 9(a). Smaller grains with no visible cellular tin precipitation in the 5Sn-95Pb samples were commonly seen throughout the joint as well as near the crack shown in Figure 9(b). Cracking in this alloy was seen to occur intergranularly.

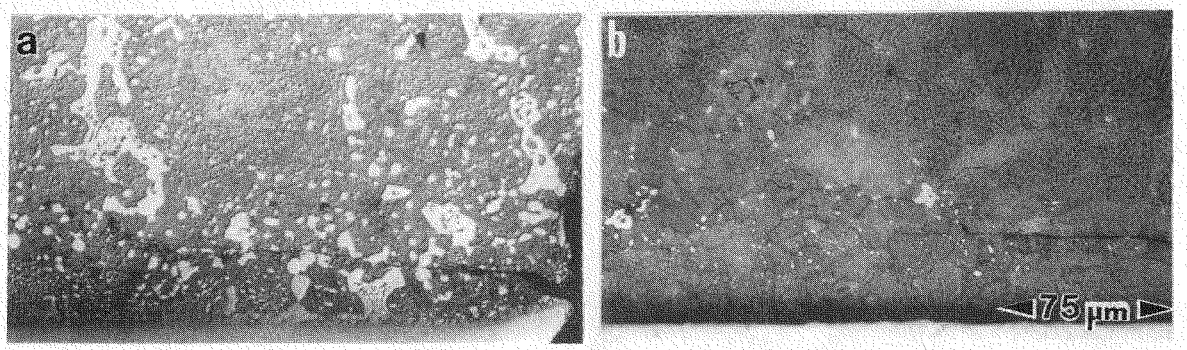

Figure 9. Micrograph of polished a)20Sn-80Pb and b)5Sn-95Pb joints that have been fatigued. (Right two figures of **XBB 898-6545**)

DISCUSSION

Fatigue Data

Of the five compositions tested 50Sn-50Pb was the most resistant to fatigue in shear. The 40Sn-60Pb, 20Sn-80Pb and 5Sn-95Pb samples had about the same resistance, and 63Sn-37Pb showed the worst fatigue resistance. This data is at least in qualitative agreement with most published data[1-4]. It has been pointed out [11] that while 5Sn-95Pb has better fatigue resistance at higher strains, 60Sn-40Pb is more resistant at smaller strains. Temperature was also found to have a stronger effect on the fatigue life of 5Sn-95Pb than on that of 60Sn-40Pb [11]. Solomon [23] also found that at room temperature, a nearly 5Sn-95Pb alloy containing a small amount of Silver had a higher Coffin-Manson coefficient than did 60Sn-40Pb resulting in better fatigue resistance at high strains and worse resistance at low strains. It is quite likely that these trends are similar for 63Sn-37Pb which behaves very similarly in fatigue to 60Sn-40Pb. Previous work in this laboratory[10] has shown 5Sn-95Pb to be inferior to 60Sn-40Pb. This discrepancy as well as the effect of strain and temperature on the relative fatigue resistance of these alloys is currently being investigated.

The fatigue lives seen here are shorter than those seen elsewhere [6,12] for similar testing conditions probably because the testing done here was done under stroke control. As discussed in detail by Solomon [5], the use of plastic strain or total strain limited testing can result in very different results. The use of plastic-strain control removes elastic machine compliance and hence the dependence of the results on the machine used for testing. Under total strain-limited testing, as the load drops during cycling, the strain applied to the solder increases. This increasing strain during cycling is most likely the reason for the relatively short lives reported here. Provided the initial loads are similar, the relative fatigue resistance measured here under stroke control should be accurate. The initial plastic strains, calculated by subtracting the previously measured machine compliance from the total stroke, were seen to be nearly the same for all tests and equal to about 10%. Interestingly, 63Sn-37Pb which had the shortest fatigue life was the strongest alloy tested and therefore had the lowest initial strain.

The effect of the increasing strain during testing can clearly be seen in Figure 4. The load drop with cycling was found to be most likely due to cracking within one or both of the joints of the specimen. This conclusion is in agreement with Solomon [5]. As shown in Figure 4, the shorter the fatigue life, the less linear the stress amplitude vs. cycle curve. Assuming the initial loads for each of the tests are nearly the same, then the shorter the life, the greater the load drop per cycle. Greater load drops are accompanied by greater increases in strain which would cause the cracking rate per cycle to increase with cycling.

The plastic strains used here were high enough to give a continuous monotonic drop in load with cycling. At smaller strains and lower temperatures, however, the load should stabilize and remain constant for a number of cycles before beginning to drop. While the load is constant, the applied plastic strain on the solder joint is constant, and Bae et al. [24] have shown that the fatigue life defined as the point where the load begins to drop is

independent of the machine compliance and only depends on the plastic strain amplitude. Current work at this laboratory involves the use of strains and temperatures which will yield this type of loading.

Failure Mechanisms

Failure of specimens with large amounts of eutectic (63Sn-37Pb, 50Sn-50Pb and 40Sn-60Pb) occurred by the coarsening mechanism observed previously in near-eutectic alloys[9,10,14-17,19]. Figure 10 shows a representative micrograph of a region within a coarsened band which is typical of those formed in these alloys. The microstructure is equiaxed and resembles a recrystallized microstructure [15]. The addition of proeutectic Pb in 50Sn-50Pb and to a lesser extent in 40Sn-60Pb had a beneficial effect on the fatigue resistance. A break up of the colony structure accompanying the addition of proeutectic was observed in 50Sn-50Pb and more so in 40Sn-60Pb (Figure 2). The smaller colony size and the more globular and coarser microstructure within the colonies was seen to delocalize the deformation of these alloys (Figure 6). Assuming the coarsened band initiation and propagation mechanisms proposed previously [16] operate in fatigue, this delocalization could postpone or even prevent formation of the coarsened band. Because the load began dropping from the beginning of testing even in the 50Sn-50Pb specimens and because significant cracking was never seen outside of a coarsened band, it is unlikely that initiation of the coarsened band was even postponed in the 40Sn-60Pb and 50Sn-50Pb alloys. Propagation of this coarsened band, however, may have occurred at a slower rate than in the eutectic specimens.

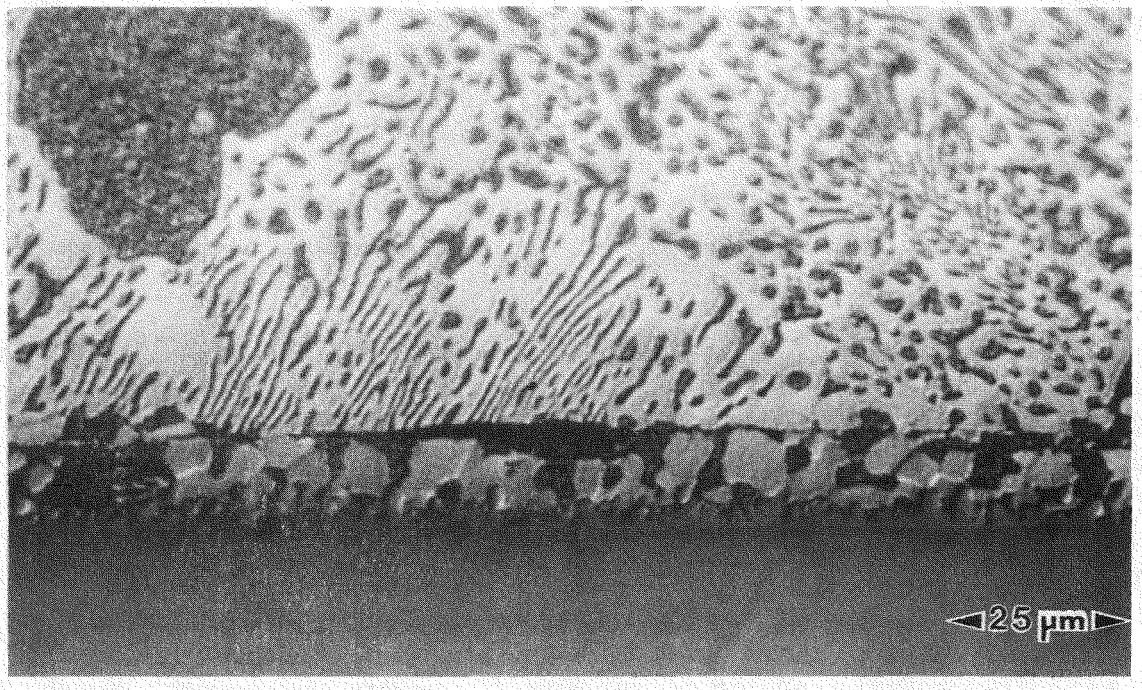

Figure 10. High magnification micrograph showing the microstructure within a coarsened band that has formed in a fatigued 40Sn-60Pb joint. This microstructure is typical of coarsened bands in all the eutectic-rich alloys tested. (**XBB 898-6768**)

Because 40Sn-60Pb has more proeutectic than 50Sn-50Pb and hence more colony break up, this delocalization of the strain cannot be the only reason for the improved fatigue resistance over 63Sn-37Pb. The proeutectic itself must play a major role in inhibiting propagation of the coarsened band probably by preventing or at least postponing recrystallization within it. The Sn precipitation observed optically may be the cause of this resistance to recrystallization. Due to nonequilibrium cooling, the Sn-content of the proeutectic in the 40Sn-60Pb alloy will be less than that in the 50Sn-50Pb alloy. Hence, the amount and distribution of Sn precipitates within the proeutectic will depend on alloy composition. Concerning the effectiveness of the proeutectic enhancing the fatigue life of the eutectic-rich alloys, then, there appears to be a trade off: decreasing the Sn content from the eutectic composition while increasing the amount of Pb-rich proeutectic, decreases the amount of Sn within the proeutectic and hence its effectiveness at inhibiting propagation of the coarsened band in eutectic-rich alloys. Ongoing research is aimed at determining the details of the effect of the proeutectic.

Cracking within coarsened regions of failed eutectic-containing specimens appears to follow regions of high area fraction of the Pb phase as shown in Figures 8(a) and (b). This observation can be interpreted in one of two ways. Either the Pb phase or the Sn phase present in areas of high Pb phase content cracks first. Figure 8(c), which is an SEM micrograph and therefore has contrast in reverse to optical micrographs, shows the end of a representative crack in a coarsened region. As is typical, this crack ends at a Pb phase boundary suggesting that the second of the above two interpretations is correct. Further research toward reaching a conclusion on this subject is currently in progress.

Failure mechanisms in the 20Sn-80Pb and 5Sn-95Pb alloys are not as straightforward as the mechanism discussed above. The microstructure shown in Figure 9(a) suggests that cracking in the 20Sn-80Pb alloy requires the local break up of eutectic material ahead of the crack tip. Details of the failure in 5Sn-95Pb are not as obvious. Two aspects of the microstructures of Figure 9(b) as compared to the initial microstructure of Figure 3(b), however, are worth mentioning. First, the overall grain size of the material appears to have decreased. Also, some regions in Figure 9(b) have relatively small grain size while others have large grains. This type of grain size distribution is what would be expected in the presence of recrystallization. Second, within some of the grains of the deformed specimen of Figure 9(b), the cellular Sn precipitates present in the as-cast structure are missing. The above observations and their effect on the fatigue resistance of these alloys is currently under investigation.

CONCLUSIONS

Of the five compositions tested, the 50Sn-50Pb solder showed the best resistance to isothermal fatigue in shear for a 10% strain amplitude, a 0.01mm/min displacement rate ($1.5 \times 10^{-4} s^{-1}$ strain rate) and a temperature of 75°C. Solders containing 5, 20 and 40% Sn had about the same fatigue resistance and were better than the eutectic (63Sn-37Pb) alloy. Failure in the eutectic, 50Sn-50Pb and 40Sn-60Pb alloys occurred by the growth of a band of coarsened material as has been seen previously in near-eutectic alloys. The addition of Pb proeutectic in the 50Sn-50Pb and 40Sn-60Pb alloys changed the microstructure in such

a way as to cause the deformation to be much more uniform than was seen in the eutectic sample. It was reasoned that a delocalization of the strain might postpone failure by a mechanism involving the formation of a coarsened region. Because the 40Sn-60Pb alloy showed more uniform deformation than the 50Sn-50Pb , it was proposed that the proeutectic itself somehow interfered with propagation of the coarsened band. Because cooling from the melt was nonequilibrium, there would have been less Sn in the 40Sn-60Pb than in the 50Sn-50Pb proeutectic. This lower Sn content might reasonably be expected to reduce the effectiveness of the proeutectic at inhibiting fatigue failure even though there is more of it. The exact effect of the proeutectic is currently under investigation. Cracking within a coarsened band was observed to follow regions with a large area fraction of the Pb-rich phase. Failure of 20Sn-80Pb appeared to initiate in the Pb phase and propagate through the eutectic regions only once the latter had broken up, and failure of the 5Sn-95Pb alloy seemed to be accompanied by a partial recrystallization and a break up or resolution of the cellular precipitates present in the as-cast alloy. Conclusions on the failure mechanisms in these two Pb-rich alloys, however, were postponed until further work could be completed.

Acknowledgement. This work was supported by the Director, Office of Energy Research, Office of Basic Energy Sciences, U.S. Department of Energy, under Contract No. DE-AC03-76SF00098.

REFERENCES

1. E.R. Bangs and R.E. Beal, "Effect of Low-Frequency Thermal Cycling on the Crack Susceptibility of Soldered Joints," Welding Research Suppl., *Welding Journal*, 54(1978), 377s-383s.

2. R.N. Wild, "Some Fatigue Properties of Solders and Solder Joints," IBM Technical Paper No. 74Z000481 (1975).

3. D.M. Jarboe, "Thermal Fatigue Evaluation of Solder Alloys," Technical Communications Bendix Kansas City: BDX-613-2341 (February, 1980).

4. H. Inoue, Y. Kurihara and H. Hachino, "Pb-Sn Solder for Die Bonding of Silicon Chips," IEEE Trans. *Components, Hybrids, and Manufacturing Technology*, CHMT-9(1986), 190-194.

5. H.D. Solomon, "Low Cycle Fatigue of 60/40 Solder - Plastic Strain Limited vs. Displacement Limited Testing," Electronic Packaging: Materials and Processes, ed. J.A. Sartell, ASM (1985), 29-48.

6. H.D. Solomon, "Fatigue of 60/40 Solder," IEEE Trans. *Components, Hybrids, and Manufacturing Technology*, CHMT-9 (1986), 423-432.

7. H.D. Solomon, "The Influence of Hold Time and Cycle Wave Shape on the Low Cycle Fatigue of 60/40 Solder," Proceedings of the 38th Electronic Components Conference, IEEE (1988), 7-13.

8. H.D. Solomon, "Strain-Life Behavior in 60/40 Solder," Presented at ASME (Nov., 1988).

9. D. Frear, D. Grivas, M. McCormack, D. Tribula and J.W. Morris, Jr., "Fatigue and Thermal Fatigue of Pb-Sn Solder Joints," Effect of Load and Thermal Histories on Mech. Behavior, TMS (1987), 113-126.

10. M. McCormack, "Initial Research Regarding Isothermal Shear Fatigue of Solder Joints," MS Thesis, University of California, Berkeley, CA, (1984).

11. M. Kitano, T. Shimizu, T. Kumazawa and Y. Ito, "Statistical Fatigue Life Estimation: The Influence of Temperature and Composition on Low-Cycle Fatigue of Tin-Lead Solders," Statistical Research on Fatigue and Fracture, *Current Japanese Materials Research*, vol. 2(1987), ed. by T. Tanaka, S. Nishijima and M. Ichikawa, Elsevier Applied Science, NY, 235-250.

12. H.D. Solomon, "Low-Frequency, High-Temperature Low Cycle Fatigue of 60Sn-40Pb Solder," ASTM-STP 942(1987), ed. by H.D. Solomon et al., 342-370.

13. W.M. Wolverton, "The Mechanisms and Kinetics of Solder Joint Degradation," *Brazing and Soldering*, 13(1987), 33-38.

14. J.W. Morris, Jr., D. Grivas, D. Tribula, T. Summers and D. Frear, " Research on the Mechanism of Thermal Fatigue in Near-Eutectic Pb-Sn Solders," 13th Annual Electronics Manufacturing Seminar Proceedings, NWC TP 6986 (March, 1989), 275-279. Also to be published in *Soldering and Surface Mount Technology*, (Sept./Oct., 1989).

15. D. Tribula, D. Grivas, D.R. Frear and J.W. Morris, Jr., "Microstructural Observations of Thermomechanically Deformed Solder Joints," to be published in Welding Research Supplement, *Welding Journal*(Oct, 1989).

16. D. Tribula, D. Grivas, D.R. Frear and J.W. Morris, Jr., "Observations on the Mechanisms of Fatigue in Eutectic Pb-Sn Solder Joints," Trans. ASME *Journal of Electronic Packaging*, 111(1989), 83-89.

17. D.R. Frear, D. Grivas and J.W. Morris, Jr., "Thermal Fatigue in Solder Joints," *Journal of Metals*, 40(1988), 18-22.

18. "Know Your Enemy: How to Stop Solder Joints from Cracking," Conference Report, *Circuits Manufacturing*, (Nov, 1972), 10-18.

19. D. Frear, D. Grivas, M. McCormack, D. Tribula and J.W. Morris, Jr., "Fatigue and Thermal Fatigue Testing of Pb-Sn Solder Joints, Proc. 3rd Ann. Electronic Packaging and Corrosion in Microelectronics Conf., 3(1987), ASM, 269-276.

20. R.C. Gifkins, "Chemical Polishing of Pb and Its Alloys," *Metallurgia*, 63(1961), 209-210.

21. R.M. Slepian and G.A. Blann, "Improved Preparation of Pb and Pb Alloys," *Metallography*, 12(1979), 353-356.

22. H.J. Frost, G.J. Stone and R.T. Howard, "The Effects of Thermal History on the Microstructure and Mechanical Properties of Solder Alloys," Micro Electronic Packaging Technology: Materials and Processes, ed. by W.T. Shieh, ASM, (1989), 121-127.

23. H.D. Solomon, "Room Temperature Low Cycle Fatigue of a High Pb Solder (Indalloy 151)," Micro Electronic Packaging Technology: Materials and Processes, ed. by W.T. Shieh, ASM, (1989), 135-146.

24. K. Bae, A.F. Sprecher, Z. Guo, H. Conrad and D.Y. Jung, "Effect of Compliance on the Fatigue of Solder Joints in Surface-Mounted Electronic Packages," Micro Electronic Packaging Technology: Materials and Processes, ed. by W.T. Shieh, ASM, (1989), 109-119.